Drug Design, Development and Therapy

Dovepress
Taylor & Francis Group

Open Access Full Text Article

ORIGINAL RESEARCH

MK-4 Ameliorates Diabetic Osteoporosis in Angiogenesis-Dependent Bone Formation by Promoting Mitophagy in Endothelial Cells

Fan Ding[1,2], Weidong Zhang[1,2], Ting Liu[1,2], Xing Rong[1,2], Yajun Cui[1,2], Lingxiao Meng[1,2], Luxu Wang[1–3], Bo Liu[4], Minqi Li[1,2,4]

[1]Department of Bone Metabolism, School and Hospital of Stomatology, Cheeloo College of Medicine, Shandong University & Shandong Key Laboratory of Oral Tissue Regeneration & Shandong Engineering Research Center of Dental Materials and Oral Tissue Regeneration & Shandong Provincial Clinical Research Center for Oral Diseases, Jinan, People's Republic of China; [2]Center of Osteoporosis and Bone Mineral Research, Shandong University, Jinan, People's Republic of China; [3]School of Stomatology, Jinzhou Medical University, Jinzhou, People's Republic of China; [4]School of Clinical Medicine, Jining Medical University, Jining, People's Republic of China

Correspondence: Bo Liu, School of Clinical Medicine, Jining Medical University, Jining, 272067, People's Republic of China, Tel +86-0537-6051782, Email liubo7230@mail.jnmc.edu.cn; Minqi Li, Department of Bone Metabolism, School and Hospital of Stomatology, Cheeloo College of Medicine, Shandong University & Shandong Key Laboratory of Oral Tissue Regeneration & Shandong Engineering Research Center of Dental Materials and Oral Tissue Regeneration & Shandong Provincial Clinical Research Center for Oral Diseases, No. 44-1 Wenhua Road West, Jinan, 250012, People's Republic of China, Fax +86-531-8838 2923, Email liminqi@sdu.edu.cn

Purpose: Diabetic osteoporosis (DOP), one of the usual complications in diabetic patients, poses a significant threat to bone health. Type H vessels in metaphysis and medial cortical bone are associated with osteogenesis. As a form of Vitamin K_2, menaquinone-4 (MK-4) is a potential treatment for osteoporosis. We aimed to investigate whether MK-4 ameliorates DOP by promoting bone formation through protecting type H vessels and its associated mechanisms.

Methods: High fat diet (HDF) feeding and streptozotocin (STZ) injection were applied to establish a mouse model of type 2 diabetic osteoporosis (T2DOP). Micro-CT, Masson staining, HE staining and IHC staining were applied to observe bone mass and the osteoblastic ability of osteoblasts. Tissue immunofluorescence (IF) staining and flow cytometry were employed to assess alteration of type H blood vessels. In vitro, to evaluate the functional level and mitophagy of ECs under high glucose conditions, wound healing assay, tube formation assay, EdU assay and IF were employed. Osteogenic differentiation ability in vitro was evaluated by ALP staining, AR staining, Western blot and RT-qPCR.

Results: MK-4 alleviated type H vessel injury and angiogenesis-dependent osteogenesis in DOP mice, thereby maintaining the bone mass. The vitro results showed that MK-4 could mitigate the dysfunction of ECs subjected to HG treatment, and further facilitate the osteogenic differentiation of MC3T3-E1 cells. Moreover, mechanism exploration found that PINK1/Parkin-mediated mitophagy was required for the impact of MK-4 on ECs. Meanwhile, ERK signal pathway is necessary for the improvement of MK-4 in PINK1/Parkin-mediated mitophagy.

Conclusion: MK-4 is capable of alleviating the PINK1/Parkin-mediated mitophagy of ECs via the ERK pathway, thereby facilitating angiogenesis-dependent bone formation and further ameliorating DOP.

Keywords: Menaquinone-4, diabetic osteoporosis, type H vessels, angiogenesis-dependent osteogenesis, PINK1/Parkin-dependent mitophagy

Introduction

As a metabolic disease, diabetes mellitus is a charactered by elevated blood glucose levels, which result from either insulin resistance or insufficient secretion of insulin.[1] With changes in diet and lifestyle, the worldwide incidence of diabetes has been rising rapidly.[2] According to international statistics from 2017, over 425 million people have been diagnosed with diabetes worldwide, and this number is projected to increase by 156% by 2045.[3] Persistent hyperglycemia causes a variety of harm to the body, including the skeletal system.[4–6] As a common complication of diabetes,

Received: 30 December 2024
Accepted: 8 March 2025
Published: 25 March 2025

diabetic osteoporosis (DOP) is marked by a decrease in bone mineral density, reduction of bone quality and an increased risk of fractures.[7,8] Previous evidence have identified that individuals with diabetes have a 20–30% greater risk of fractures compared to those without diabetes.[9] Once the fracture occurs, the patient's quality of life can be severely impacted, and in some cases, it may lead to death.[10] However, there are currently no effective treatments available. Developing effective therapies for DOP holds significant economic and social importance.

Vascular damage caused by diabetes is extensive and severe, encompassing nearly all types and magnitudes of blood vessels, such as coronary arteries, retinal blood vessels, and renal microvessels.[11–13] Skeletal system is a highly vascularized tissue and endothelial cells (ECs) play essential roles in osteogenesis and hematopoiesis.[14] Kusumbe found a new specific category of blood vessel in the metaphysis and medial cortical bone, known as type H blood vessel, which is characterized by high expression of CD31 and endomucin (Emcn) in ECs.[15] Due to its unique morphology and function, type H vessels are integral to both osteogenesis and angiogenesis.[16] Factors such as vascular endothelial growth factor (VEGF), Notch, hypoxia-inducible factor 1-α (HIF-1α), slit guidance ligand 3 (SLIT3) and platelet-derived growth factor-BB (PDGF-BB), have been identified to serve a key role in coupling of osteogenesis and angiogenesis.[15] Tissue engineering research also proves that the absence of type H vessels can inhibit osteogenesis in regenerative tissues.[16] Therefore, the coupling relationship between angiogenesis and bone formation has become a breakthrough point in the treatment of osteoporosis. In recent years, it has been shown that diabetic mice have reduced bone-type H vessels and impaired coupling of angiogenesis and osteogenesis.[17] Therefore, targeting the mechanism of angiogenesis-osteogenesis may be a potential therapeutic strategy for DOP.

Vitamin K_2 (VK_2) is a lipophilic vitamin, also known as menaquinone (MK), which occurs naturally mainly in animal-based foods and specific fermented and is commonly available in Vitamin K supplements.[18] As a form of VK_2, menaquinone-4 (MK-4) has four isoprenoid residues in its side chain.[19] Studies have demonstrated MK-4 treatment reduces bone loss in mice following ovariectomy and decreases osteoporotic fractures in postmenopausal women.[20,21] Another study reported that MK-4 alleviates bone loss through the improvement of osteoblast function in rats.[22] Additionally, our previous research has demonstrated that MK-4 can suppress osteoblast apoptosis.[23] These findings suggest that MK-4 has positive effects on promoting bone formation. Moreover, VK_2 has long been regarded as a cardioprotective and vasculoprotective agent, as it effectively inhibits the calcification of heart valves and blood vessels.[24] Studies have shown that VK_2 improves $ApoE^{-/-}$ mice's nitric oxide-dependent activity of endothelial cells.[25] Furthermore, VK_2 has been reported to enhance angiogenesis and improve blood vessels in femoral head of rats treated with glucocorticoids.[26] Considering the coupling between angiogenesis and osteogenesis, along with biological function of Vitamin K_2, we hypothesize that MK-4 ameliorates DOP by promoting bone formation by protecting type H vessels.

A murine model of type 2 diabetes osteoporosis (T2DOP) was created in this research to investigate impacts of exogenous MK-4 on type H vessels and its involvement in bone loss associated with diabetes. Furthermore, our attention was directed towards the mitophagy mediated by the PINK1/Parkin pathway, which is regulated by extracellular signal-regulated kinase (ERK) signaling, in order to investigate the relevant mechanisms through which MK-4 alleviates ECs dysfunction and promotes angiogenesis-dependent bone formation. The objective of this research is to explore how MK-4 protects against diabetic osteoporosis and to uncover the mechanisms involved, providing a new therapeutic approach for diabetic complications.

Materials and Methods

T2DOP Model Establishment, Treatment and Tissue Preparation

Jinan Pengyue Laboratory Animal Breeding Co., Ltd. (Jinan, China) supplied the male C57 BL/6 mice. The study involved 20 male C57 BL/6 mice, randomly divided into four groups (n=5 per group): the wild-type (WT) group, the DOP group, the DOP + MK-4 group and the DOP + MK-4 + 3-MA group. To establish a T2DOP mouse model, the animals were provided with a high-sugar and high-fat diet for 4 weeks, followed by intraperitoneal injection of streptozotocin (STZ).[27] Mice with fasting blood glucose levels consistently exceeding 11.1 mmol/L for more than 7 days, following one week of alternate-day STZ injections, and showing impaired insulin sensitivity were confirmed to be diabetic and included in subsequent studies. Blood glucose levels and body weight were recorded weekly throughout the

study. Mice in the DOP + MK-4 group received oral supplementation with MK-4 (30 mg/kg; Glakay, Shibakawa Plant of Fuji Capsule Co., Ltd., Japan) five times per week for eight weeks. WT and DOP groups were given glycerol as a placebo. Meanwhile, as the aim of administering 3-Methyladenine (3-MA; Cat. No. HY-19312) is to block the autophagy-promoting effect of MK-4, intraperitoneal injection of 3-MA at a dosage of 15 mg/kg was administered to the DOP + MK-4 + 3-MA group five times per week for a total of eight weeks.[28] Mice in the WT group and DOP group were given normal saline as a blank control. The mice were numbed and immobilized using intracardiac perfusion of 4% paraformaldehyde following the treatment. The tibias were extracted after fixation and immersed in the external fixation fixative. And after that, for four weeks, the tibias were placed in an EDTA solution at 4 °C for decalcification. Following treatment with a gradient series of ethanol or a 20% sucrose solution for dehydration, the tissues were either embedded in paraffin and sliced into 5 μm thick slices or embedded in optimal cutting temperature compound (O.C.T., Aoqing Biotechnology Co., Ltd., Beijing, China) and sliced into 40 μm thick frozen slices for histological analysis.

Immunofluorescence (IF) Staining

Firstly, immerse the 40 μm-thick frozen slices in double-distilled water for 10 minutes to completely dissolve O.C.T. After that, it was permeabilized with 1% Triton X-100 for half an hour and blocked with 1% BSA-PBS for the same amount of time. The same procedure was used to fix the endothelial cells (ECs): 4% paraformaldehyde (PFA), 0.5% Triton X-100, and 5% BSA in PBS. Afterwards, the specific mixed antibodies were applied to the tissue slices or cells and left to incubate overnight at 4 °C. These antibodies included: anti-CD31 (ab9498, Abcam, Cambridge, UK), anti-Endomucin (ab106100, Abcam), anti-Osterix (ab209484, Abcam), anti-LC3B (14600-1-AP, Proteintech), anti-COXIV (11242-1-AP, Proteintech), and anti-P62/SQSTM1 (18,420-1-AP, Proteintech). The nuclei were labeled the following day by exposing them to 4′,6-diamidino-2-phenylindole (DAPI) after an hour of room temperature exposure for 5 minutes to fluorescent secondary antibodies. One last step was to use a confocal microscope to look at the cells or tissue slices.

Flow Cytometry

To analyze the quantity of $CD31^{hi}Emcn^{hi}$ cells in the bones of mice in each group, mouse femurs were isolated following the removal of the surrounding muscles and periosteum. After the metaphysis was cut off, the bone marrow cavity was flushed with 1 mL of ice-cold PBS. After centrifugation, the crushed metaphysis, diaphysis, and cell precipitate were treated with collagenase (ST2303, 0.5 mg mL^{-1}; Beyotime Institute of Biotechnology, Shanghai, China), and a single-cell suspension was obtained after sieving. Subsequently, red blood cells were lysed using red blood cell lysis buffer (Solarbio, R1010) according to the specified procedures. After filtration and washing, the cells were incubated with an endomucin antibody (sc-65495, Santa) at 4 °C for 45 minutes, after that, it is washed and then incubated utilizing a fluorescent secondary antibody conjugated with FITC for 40 minutes. The cells were subsequently washed and later incubated with PE-conjugated CD45 (E-AB-F1136D, 1:20; Elabscience, Wuhan, China) and APC-conjugated CD31 (E-AB-F1180E, 1:20; Elabscience) antibodies at 4 °C for 45 minutes. Data acquisition was conducted using a flow cytometer.

Bone Mass Measurement

Following the fresh dissection of tibias, the bone microstructural parameters of the proximal tibias were analyzed with the Micro-CT scanner (SCANCO Medical AG, Bruttisellen, Switzerland). Next, following the dewaxing and hydration of the paraffin slices with a thickness of 5 μm, which were obtained after the treatment described earlier, the Hematoxylin and Eosin (HE) staining and Masson staining procedures were conducted based on the established protocols. In the following step, the slices were mounted after being dehydrated. An optical microscope (Olympus BX-53, Tokyo, Japan) was to obtain the images. Image Pro Plus 6.2 software was utilized to quantify the trabecular separation (Tb. Sp), trabecular number (Tb. N), trabecular thickness (Tb. Th) and parameters of trabecular bone volume (BV/TV).

Immunohistochemical Staining (IHC)

To inhibit the activity of endogenous peroxidase, the treated sections were immersed in a PBS solution that contained 0.3% hydrogen peroxide for a period of thirty minutes. Then, they were treated with 1% bovine serum albumin (BSA) in

PBS for twenty mins. This was followed by an overnight incubation with anti-ALP (A12396, ABclonal) and anti-RUNX2 (ab192256, Abcam). Slices were incubated with the secondary antibody for one hour at room temperature the following day. The immune reactions were identified with the help of 3.3′-diaminobenzidine tetrahydrochloride (DAB), which was manufactured by Sigma-Aldrich through Merck KGaA in Germany. Following that, each section was counterstained with methyl green, and then photographs were taken with an optical microscope (BX-53, Olympus Corporation, Japan).

Cell Counting Kit-8 (CCK-8) Assay

ECs were seeded at a density of 5×10^3 cells/well. Next, they exposed with high glucose (HG) (0, 15, 25, 35, 45, and 55 mm), MK-4 (0.1, 1, 10, 50, and 100 μM), and a combination of MK-4 with HG (35 μM/mL) for 48 hours to determine the optimal concentrations. The CCK8 (HYK0301, MedChemExpress) assay was performed by adding 10 μL of CCK-8 reagent and incubating the plate at 37°C for 1 hour. An enzyme-linked immunosorbent assay reader (iMark, Bio-Rad Laboratories, Inc). was applied to detect the result.

5-Ethynyl-2′-Deoxyuridine (EdU) Assay

In order to determine the level of cell proliferation, the BeyoClickTM EdU Cell Proliferation Kit with Alexa Fluor 594 (C0078, Beyotime) was utilized. Following the placement of endothelial cells in confocal dishes, the cells were allowed to incubate for a period of forty-eight hours. Following that, the samples were subjected to incubation at a temperature of 37 degrees Celsius for a duration of two hours using a working solution containing 10 micromolar of eugenol (EdU). Following a fixation period of fifteen minutes in 4% PFA, the cells were permeabilized with 0.3% Triton X-100 for a period of twenty minutes. After being exposed to azide 594 for thirty minutes at room temperature without light, the cells were exposed to DAPI for five minutes before being incubated with DAPI once again. Following the application of the EdU stain, the cells were subsequently examined using a confocal microscope. As a next step, the proportion of EdU-positive cells to the total number of cells was calculated.

Wound Healing Assay

3×10^5 cells/well was the concentration of ECs that was plated in a 6-well plate. After the cells had achieved 90–100% confluence, a 200 μL pipette tip was employed to make vertical scratches on the surface of the cell layer. We cultured the cells in 2% FBS-DMEM after washing them with PBS. They were then incubated and processed in accordance with the protocol. At 0, 24, and 48 hours after scratching, photos were taken using a microscope (Olympus BX53, Tokyo, Japan). The wound healing percentage was then determined employing Image-Pro Plus 6.0 software (Media Cybernetics).

Tube Formation Assay

To perform the tube formation assay, 70 μL/well of Matrigel (ABW, China) was coated on a 96-well culture plate pre-cooled to 4 °C and placed in a 37 °C cell culture incubator for 30 minutes to allow the matrix solution to solidify. The suspensions of ECs in each group, which had been treated with serum starvation for 6 hours, were seeded on solidified Matrigel in the 96-well plate with a cell density of 1.5×10^5 per well. Images were captured after incubation at 37 °C for 4 and 8 hours.

Real-Time Polymerase Chain Reaction (RT-qPCR) Analysis

The method of RT-PCR is as our previous study.[29] In brief, total RNA was extracted and reversed transcription to cDNA. The SYBR Green Pro Taq HS premixed RT-qPCR Kit (AG11701, Accurate Biotechnology (Human) Co., Ltd., China) was utilized to the expression of different genes. The expression of GAPDH was utilized to normalize all of the data, and the quantitative polymerase chain reaction (qPCR) results were analyzed by employing the $2^{-\Delta\Delta Cq}$ method for quantification. A total of five replicates of each sample were performed, and the primer sequences are presented in Table 1.

Table 1 Specific Primers for Control and Target Genes

Gene	Forward	Reverse
TGF-β	5′-GCAACAATTCCTGGCGATACC-3′	5′-ATTTCCCCTCCACGGCTCAA-3′
Noggin	5′-GCCAGCACTATCTCCACATCC-3′	5′-AAGATAGGGTCTGGGTGTTCG-3′
GAPDH	5′-AGAAGGCTGGGGCTCATTTG-3′	5′-AGGGGCCATCCACAGTCTTC-3′

Western Blotting

Similarly, the operation of Western blotting was also as previous study.[29] In short, the protein was extracted and measured the concentration. After Electrophoresis and membrane transfer, the membranes were incubated with the primary antibodies for one night at 4°C. These antibodies included: anti-GAPDH (ab9485, Abcam), anti-ALP (ab108337, Abcam), anti-RUNX2 (ab192256, Abcam), anti-LC3B (14600-1-AP, Proteintech), anti-P62/SQSTM1 (18,420-1-AP, Proteintech), anti-ERK1/2 (11,257-1-AP, Proteintech), anti-p-ERK (28733-1-AP, Proteintech), anti-Beclin 1 (11,306-1-AP, Proteintech), anti-PINK1 (WL04963, Wanleibio), anti-Parkin (WL02512, Wanleibio). At second day, second antibodies were incubated. A gel imaging system, specifically the Amersham Imager 600 from General Electric Company in Boston, USA, was utilized to acquire the images. Image-Pro Plus 6.2 (Media Cybernetics) was used to quantify and evaluate the grayscale values, which were then normalized to the levels of GAPDH. There were a minimum of five repetitions of each experiment.

Alkaline Phosphatase (ALP) Staining and Alizarin Red (AR) Staining

Seven days were spent cultivating the MC3T3-E1 cells in an osteogenic induction medium. PBS was used to wash the cells after they had been fixed with 4% paraformaldehyde for twenty minutes. Following this, the cells were incubated with ALP solution (Solarbio, Beijing, China) in accordance with the instructions provided by the manufacturer. This was followed by the utilization of optical microscopy (CKX-41, Olympus Corporation, Japan) in order to acquire the images. MC3T3-E1 cells were maintained in osteogenic induction medium for a period of 21 days in order to facilitate the formation of mineralized nodules, which was then used to evaluate the deposition of minerals. The cells were first fixed in 4% PFA, then stained with a 1% AR staining solution (Lot. No.20180820, Solarbio, China), and finally, the AR was extracted with cetylpyridinium chloride.

Evaluation of Mitochondrial Function

Mitochondrial membrane potential (MMP) was initially evaluated through JC-1 staining using instructions from the mitochondrial membrane potential assay kit with JC-1 (C2006, Beyotime). In short, the treated ECs were exposed to JC-1 dye for 30 minutes and subsequently observed under the confocal microscope. Additionally, the treated cells were exposed to a medium containing 100 nM Mito-Tracker Green (C1048, Beyotime), 5 μM MitoSOX Red (S0061, Beyotime), and Hoechst live cell staining solution (C1027, Beyotime) in confocal dishes for 30 minutes in the dark at 37°C, after which the mitochondrial superoxide generation was observed under a confocal microscope.

Transmission Electron Microscopy (TEM)

The ultrastructure of ECs was assessed by TEM. Each sample was pre-fixed with 2.5% glutaraldehyde and then subjected to a secondary fixation with 1% osmium tetroxide. Thereafter, they were dehydrated incrementally using acetone, infiltrated successively in appropriate proportions and embedded in epoxy resin. Using an ultramicrotome (UC7rt, LEICA), the samples were sectioned into thin slices. The ultrathin sections (60–90 nm), stained with uranyl acetate and lead citrate, were placed on copper grids and observed by a JEM-1400FLASH transmission electron microscope from JEOL.

Statistical Analysis

Five separate iterations of each experiment were carried out independently. For the purpose of statistical analysis, the software GraphPad Prism 6 (San Diego, California, United States) was utilized. A one-way analysis of variance (ANOVA) was utilized to evaluate the five groups, and all of the results were presented in the form of the mean plus

or minus the standard deviation (SD). In order to evaluate the differences between the groups, the Bonferroni post-hoc test was employed, with a significance level of $P < 0.05$ being considered statistically significant.

Results

MK-4 Attenuates HG-Induced ECs Dysfunction

To evaluate the cell viability under different concentrations of HG treatment and the effects of various drug concentrations on cells, gradient concentrations of HG, MK-4 and HG + MK-4 were applied to assess the viability of ECs using the CCK-8 assay (Figure 1a–c). HG made cell viability decreased in a dose-dependent manner after 48 hours and significant cytotoxicity was observed when glucose concentration exceeded 35 mmol/L (Figure 1a). In contrast, MK-4 maintained the average cell capacity for 48 hours until the concentration surpassed 10 μmol/L (Figure 1b). The combined treatment of 0.1 μmol/L or

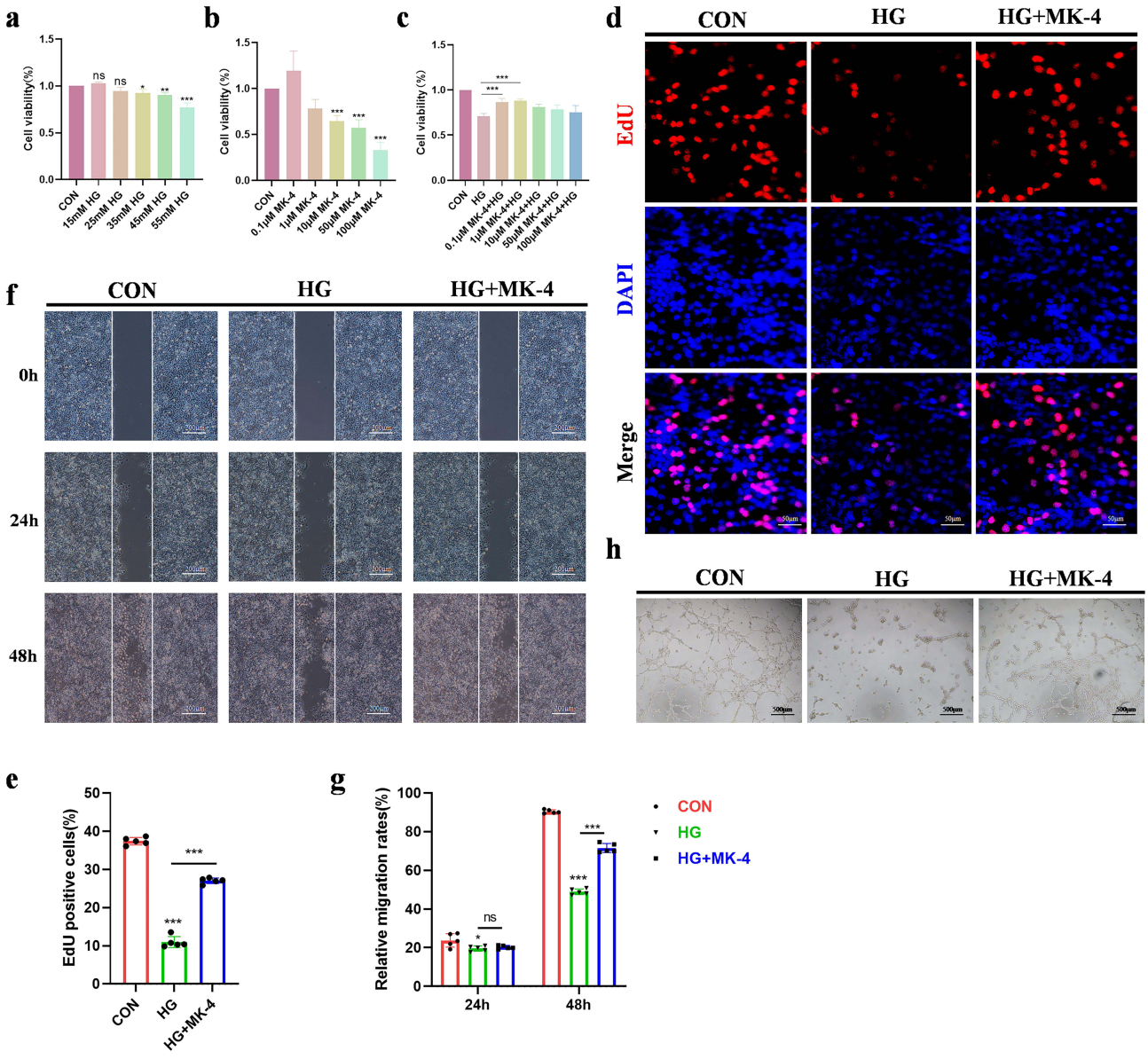

Figure 1 MK-4 attenuates HG-induced ECs dysfunction. (**a**) Cell viability of ECs cell lines treated with gradient concentrations of HG treatment for 48 hours. (**b**) Effect of MK-4 at different concentrations on the viability of ECs treated for 48 hours. (**c**) Effect of MK-4 at different concentrations for 48 hours on the viability of HG (35 mmol/L)-exposed ECs. (**d** and **e**) Representative images of EdU staining in ECs under different treatments. Scale bars, 50 μm. The bar graph showed the percentage of EdU-positive cells. (**f** and **g**) Representative images of the migration area of ECs in different treatments. Scale bar: 200 μm. The bar graph showed the quantification of the migration area of ECs in different treatments. (**h**) Representative images of tube formation in ECs stimulated with different treatments. Scale bar: 500 μm. Data given as the mean±SD were representative of five independent experiments with similar results. *$P < 0.05$. **$P < 0.01$. ***$P < 0.001$.

1 μmol/L MK-4 significantly improved cell viability of 35 mmol/L HG exposure following 48 hours and the strongest protective impact from cell toxicity was observed at 1 μmol/L MK-4 (Figure 1c). Based on these findings, 35 mmol/L HG and 1 μmol/L MK-4 were chosen for subsequent experiments. Then EdU assay demonstrated that HG significantly inhibited ECs proliferation, partially restored by MK-4 treatment (Figure 1d and e). As shown in the scratch assay (Figure 1f and g), the migratory capacity of ECs was attenuated by HG stimulation, in comparison to the control group; in contrast, the migratory capacity was partially restored following MK-4 treatment. In the investigation of the effect of MK-4 on angiogenesis under HG stimulation, as depicted in Figure 1h, in comparison with ECs treated with HG, treatment with MK-4 resulted in the formation of a more significant number of capillary-like structures on Matrigel by HG-stimulated ECs. These findings indicate that MK-4 may help alleviate EC dysfunction induced by HG.

MK-4 Ameliorates the Impairments of Type H Vessel and Angiogenesis-Dependent Osteogenesis in DOP Mice

We established an STZ-induced type 2 diabetes mouse model, with some mice receiving oral administration of MK-4 (Figure 2a). Flow cytometry analysis first demonstrated a marked reduction in the number of type H ECs in the tibias of DOP mice compared to WT mice. However, in MK-4-treated DOP mice, there was a noticeable trend towards the recovery of type H ECs numbers (Figures 2b and c). Subsequently, IF staining was performed to assess the alteration of type H vessel formation and angiogenesis-dependent bone formation in DOP mice. We observed a significant reduction of $CD31^{hi}$ $Emcn^{hi}$ type H vessels and surrounding $Osterix^{+}$ osteoprogenitor cells near the growth plate in DOP mice compared to WT mice and MK-4 treatment alleviated the reduced trend (Figure 2d–g). Micro-CT images revealed that a considerable reduction in bone density was observed in DOP mice compared to WT mice, which was notably alleviated by MK-4 treatment (Figure 2h). The HE staining results were consistent with Micro-CT findings (Figure 2i and 2j). Masson staining showed more extensive areas of new bone formation in WT mice, while DOP mice exhibited reduced new bone formation. MK-4 treatment increased the blue-stained area, suggesting MK-4 ameliorates the impaired osteogenesis in DOP mice (Figure 2i)Meanwhile, we measured the osteogenic capacity by measuring the expression of osteoblast activity markers, such as ALP and RUNX2. DOP mice exhibited significantly decreased ALP and RUNX2 expression in the metaphyseal region, whereas MK-4 treatment partially restored their levels (Figure 2k and l). These findings suggested that MK-4 protected against the impairment of type H vessels and osteogenic capacity in DOP mice.

MK-4 Ameliorates HG-Induced Angiogenesis-Dependent Osteogenesis Disorders

The interaction between ECs and the osteogenic cell lineage mediates the coupling between angiogenesis and osteogenesis. ECs regulate osteoblast activity through the paracrine secretion of factors like Noggin and TGF-β. Figure 3a demonstrates that the mRNA expression levels of Noggin and TGF-β in ECs, as determined by RT-qPCR, were significantly reduced in HG-treated cells when compared to control group. However, cells treated with both HG and MK-4 exhibited higher mRNA levels than those treated with HG alone. For the purpose of continuing to explore the function of MK-4 in enhaing osteogenesis under hyperglycemic conditions, we collected supernatants from normal glucose (NG), HG, and HG+MK-4 treated ECs and mixed them in a 1:1 ratio with osteogenic induction medium. This mixture was used to treat MC3T3-E1 cells. ALP and AR staining results revealed that conditioned medium (CM) from HG-stimulated ECs significantly suppressed the activity of ALP and the deposition of calcium in MC3T3-E1 cells compared to untreated cells. However, CM from HG-treated ECs with MK-4 co-treatment partially restored ALP activity and mineralized nodule formation in MC3T3-E1 cells (Figure 3b). The results were corroborated by Western blotting (Figure 3c and d). In summary, our result showed that MK-4 ameliorates HG-induced impairment of angiogenesis-dependent bone formation in vitro.

MK-4 Alleviates HG-Induced EC Dysfunction by Promoting Mitophagy

Mitochondria are the principal organelles suffering from high glucose. Additionally, studies have indicated that mitochondrial dysfunction is associated with the impairment of ECs.[30] The JC-1 staining result showed that the exposure of HG significantly decreased the MMP, with weak red and strong green fluorescence. In contrast, MK-4 treatment augmented the MMP of ECs

 https://doi.org/10.2147/DDDT.S503930

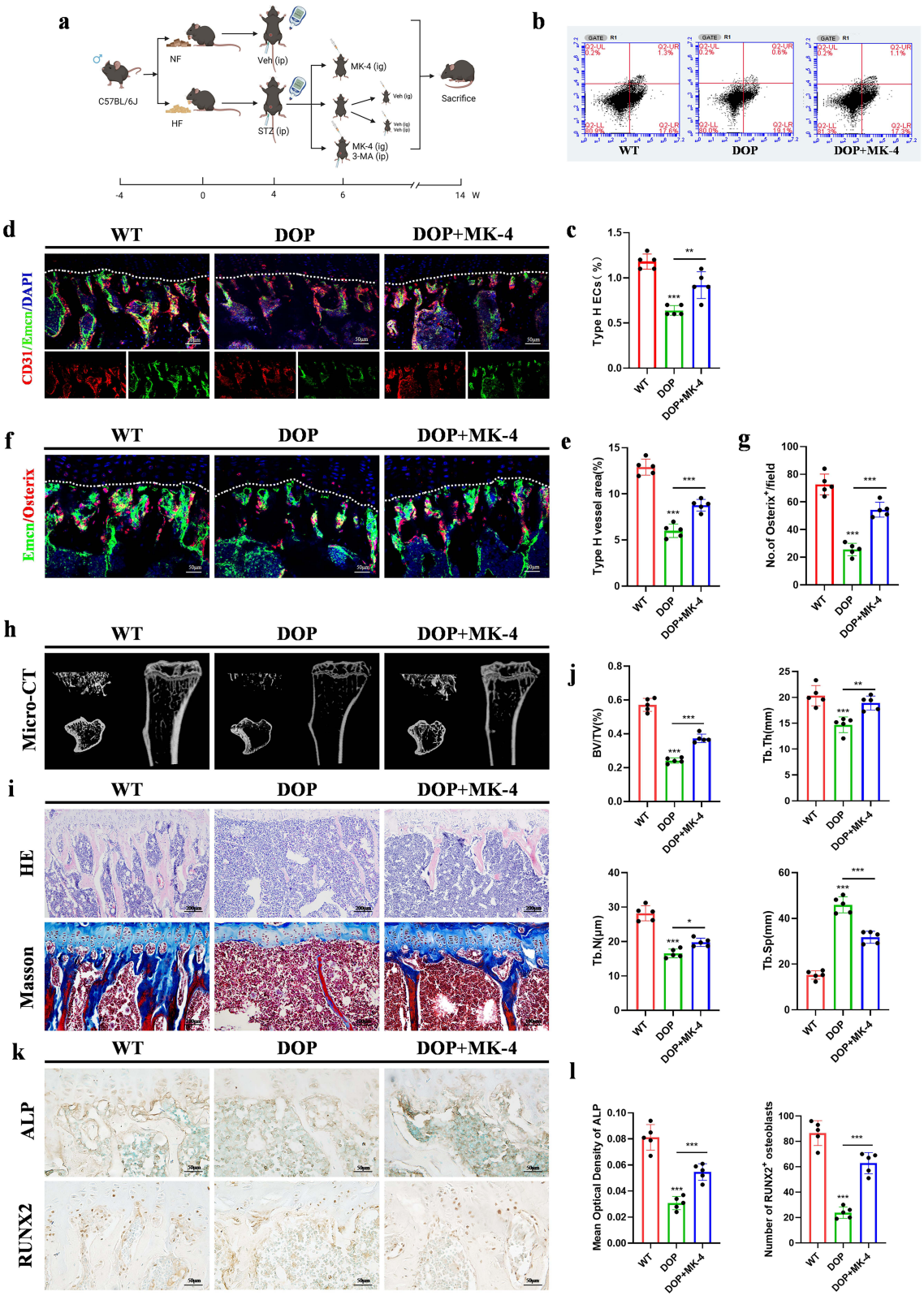

Figure 2 MK-4 ameliorates the impairments of type H vessel formation and angiogenesis-dependent bone formation in DOP mice. (**a**) Schematic drawing of the procedures conducted in this study. (**b** and **c**) Representative flow cytometry plots of CD31^{hi}Emcn^{hi} ECs (type H ECs). The bar graph showed the quantitation of type H ECs. (**d** and **e**) Confocal image of CD31^{hi} and Emcn ^{hi} (type H blood vessels) in mice models and histomorphometric quantitation of the area of type H blood vessels. Scale bar: 50μm. (**f** and **g**) Confocal image of Osterix^{+} (green) osteoprogenitors around CD31^{hi} vessels (red) and the quantitative analysis. Scale bar: 50μm. (**h**) Typical three-dimensional and two-dimensional coronal images of the tibias were obtained by Micro-CT. (**i**) HE and Masson staining of mice tibias. Scale bar: 200μm or 100μm. (**j**) Statistical analysis of bone histological parameters. (**k** and **l**) IHC analysis of ALP and RUNX2 in the tibias of mice models. Scale bar: 50μm. Data were presented as mean ± SD (n=5). *P < 0.05. **P < 0.01. ***P < 0.001.

https://doi.org/10.2147/DDDT.S503930

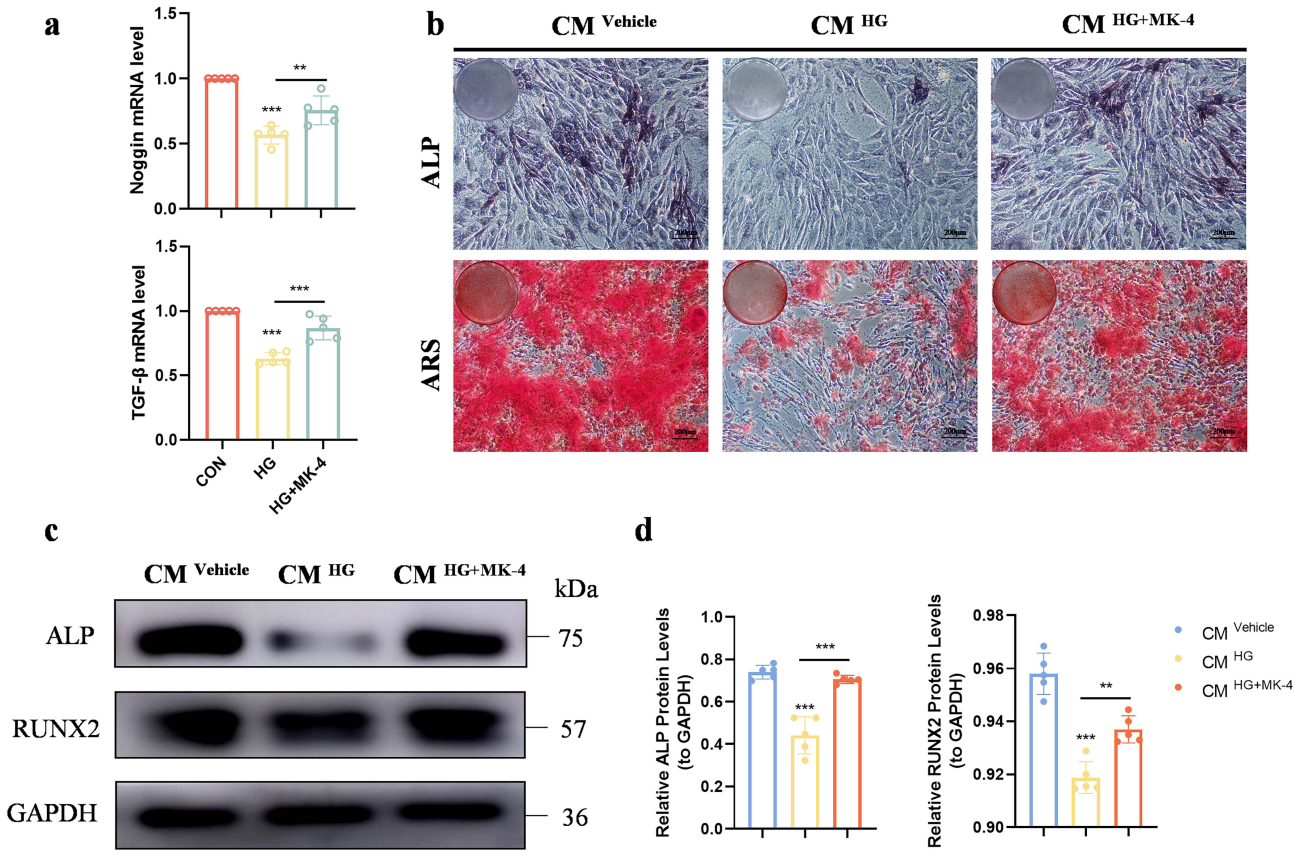

Figure 3 MK-4 ameliorates HG-induced angiogenesis-dependent bone formation disorders. (**a**) The RT-qPCR analysis of Noggin and TGF-β in each group. (**b**) ALP staining and ARS staining. (**c**) The protein expression of ALP, RUNX2, and GAPDH was detected by Western blotting. (**d**) The statistical analysis of Western blotting. Data given as the mean±SD were representative of five independent experiments with similar results. $^{**}P < 0.01$. $^{***}P < 0.001$.

impaired by HG (Figure 4a and b). MitoSOX analysis also demonstrated that HG stimulation caused mitochondrial damage, while MK-4 treatment reduced the production of mitochondrial reactive oxygen species (mtROS) induced by HG (Figure 4c and d). Subsequently, to further elucidate how HG induces mitochondrial damage to ECs, as observed via transmission electron microscopy (TEM), in comparison with the control group, HG stimulation markedly decreased the quantity of mitochondrial autophagic vacuoles, whereas MK-4 treatment augmented the number of these vacuoles (Figure 4e). In this experiment, 3-MA, a commonly used inhibitor of autophagy, was applied to block the mitophagy induced by MK-4.[28] Immunofluorescence analysis indicated that the colocalization of LC3B and mitochondria diminished under HG conditions. MK-4 treatment maintained this colocalization, whereas the addition of 3-MA partially weakened the promoting effect of MK-4 (Figure 4f and g). Consistently, the upregulation of the colocalization between P62/SQSTM1 and mitochondria following HG stimulation was reversed under the treatment of MK-4, whereas 3-MA attenuated this effect (Figure 4h and i). Further analysis of MMP and mtROS indicated that MK-4 treatment improved MMP and reduced mtROS compared to the HG group, indicating a comprehensive enhancement in mitochondrial function. Nevertheless, the mitochondrial protective effect of MK-4 was diminished by 3-MA, indicating that mitophagy may be crucial for MK-4's enhancement of mitochondrial adaptation (Figure 4j–m). Subsequently, upon applying 3-MA, the functions of ECs regarding proliferation, migration, and tube formation were assessed. It was discovered that the application of the autophagy inhibitor partially counterbalanced the protective effect of MK-4 on the functions of ECs (Appendix Figure 1a-e). These data suggested that MK-4 alleviates HG-induced ECs dysfunction by promoting mitophagy.

3-MA Partially Counteracts the Promotion of Type H Vessel Recovery and Angiogenesis-Dependent Bone Formation Gain by MK-4

Next, we assessed the involvement of mitophagy in the protective action of MK-4 in a DOP mouse model. 3-MA was injected into a subset of MK-4-treated DOP mice, and comparisons were made with DOP mice and MK-4-treated groups.

https://doi.org/10.2147/DDDT.S503930

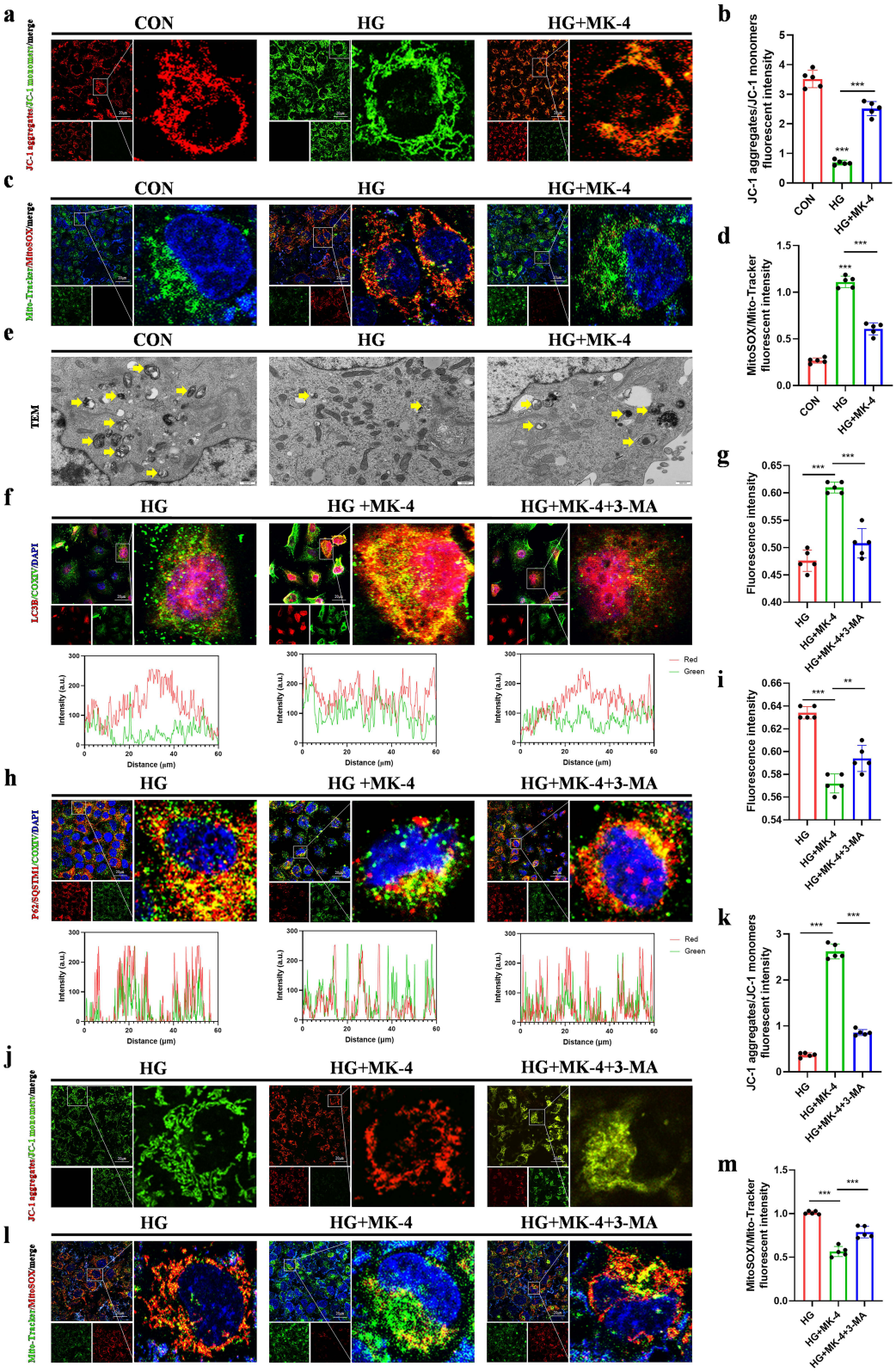

Figure 4 MK-4 alleviates HG-induced EC dysfunction by promoting mitophagy. (**a** and **b**) Fluorescence staining of JC-1 showed mitochondrial membrane potential in the CON, HG and HG+MK-4 groups. Scale bar: 20μm. (**c** and **d**) The assessment of MitoSOX. Scale bar: 20μm. (**e**) The TEM to observe the alteration of mitophagy vacuoles. Mitophagy vacuoles are captured as pointed yellow triangles. (**f** and **g**) IF staining of LC3B and COXIV to assess the alteration of mitophagy. Scale bar: 20μm. (**h** and **i**) IF staining of P62/SQSTM1 and COXIV to assess the alteration of mitophagy. Scale bar: 20μm. (**j**–**m**) The assessment of mitochondrial membrane potential and MitoSOX to identify the role of mitophagy. Scale bar: 20μm. Data given as the mean±SD were representative of five independent experiments with similar results. $^{**}P < 0.01$. $^{***}P < 0.001$.

Immunofluorescence staining showed that 3-MA co-treatment diminished MK-4's beneficial effects on type H vessels and the number of Osterix^{+} osteoblast progenitor cells surrounding the vessels in DOP mice (Figure 5a–d). Bone volume assessments revealed that 3-MA co-treatment blocked MK-4's protective effect against bone loss in DOP mice, suggesting that mitophagy partially mediates MK-4's protective action (Figure 5e–h). In conclusion, mitophagy played a crucial role in the effect of MK-4 on protecting type H vessels and promoting angiogenesis-dependent bone formation.

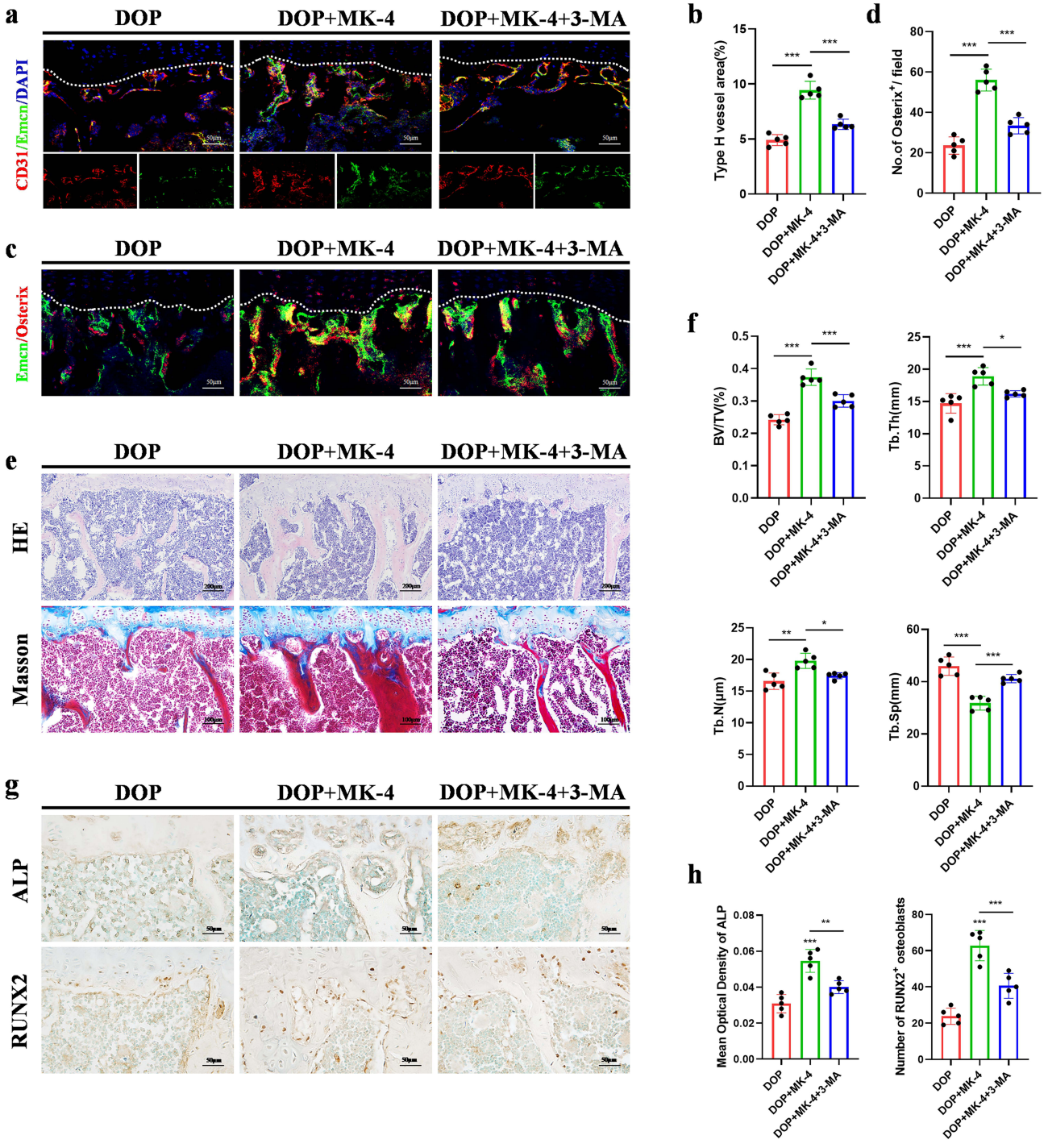

Figure 5 3-MA partially counteracts the promotion of type H vessel recovery and angiogenesis-dependent bone formation gain by MK-4. (**a** and **b**) Confocal image of CD31^{hi} and Emcn ^{hi} (termed type H blood vessels) in mice models and histomorphometric quantitation of the area of type H blood vessels. Scale bar: 50μm. (**c** and **d**) Confocal image of Osterix^{+} (red) osteoprogenitors around Emcn^{hi} vessels (green) and the quantitative analysis. Scale bar: 50μm. (**e**) HE and Masson staining of mice tibias. Scale bar: 200μm or 100μm. (**f**) Statistical analysis of bone histological parameters. (**g** and **h**) IHC analysis of ALP and RUNX2 in the tibias of mice models. Scale bar: 50μm. Data were presented as mean ± SD (n=5). *P < 0.05. **P < 0.01. ***P < 0.001.

https://doi.org/10.2147/DDDT.S503930

MK-4 Promotes PINK1/Parkin-Mediated Mitophagy to Alleviate ECs Dysfunction via the ERK Signaling Pathway

We conducted further investigations to explore the specific mechanism through which MK-4 regulates mitophagy in ECs. The ERK 1/2 signaling pathway is considered to be essential for the regulation of autophagy.[31] Western blot analysis revealed a significant decrease in ERK phosphorylation levels in the HG stimulation group compared to the CON group. In comparison, the MK-4 treatment group exhibited higher P-ERK expression than the HG group (Figure 6a and b). The remaining total ERK expression implies that MK-4 promotes ERK phosphorylation. To investigate the involvement of ERK 1/2 in the protective mitophagy induced by MK-4, we employed U0126 which selectively inhibits the phosphorylation of components in the ERK signaling pathway to suppress ERK 1/2 phosphorylation. The results from Western blot analysis indicated that inhibiting the phosphorylation of ERK 1/2 resulted in decreased expression of LC3B and Beclin 1, while blocking the degradation of P62/SQSTM1, suggesting that MK-4-induced formation and degradation of autophagosomes rely on the ERK 1/2 pathway (Figure 6c and d). We then examined how inhibiting ERK 1/2 affects mitophagy. Both IF and Western blot analyses indicated that inhibition of the ERK 1/2 signaling pathway prevented the MK-4-induced upregulation of PINK1 and Parkin levels (Figure 6c–f). The evidences suggest that the ERK 1/2 signaling pathway may be essential for MK-4 to regulate PINK1/Parkin-mediated mitophagy.

Discussion

Our study found that MK-4 could promote type H vessels and angiogenesis-dependent bone formation by attenuating HG-induced ECs dysfunction, and thus partially restoring bone mass in DOP mice. We also found that mitophagy is necessary for the protective role of MK-4. Our study enriches the theoretical basis of MK-4 treatment for DOP and provides novel insight for further targeting the regulation of angiogenesis-dependent bone formation in DOP pathogenesis. In the past few decades, we have made significant progress in understanding molecular and cellular mechanisms of DOP progression as well as investigated some drugs to treat DOP. In this study, we identified the influential role of MK-4 in DOP. It was well known that MK-4, as a variant of VK_2, can activate γ-carboxylation of osteocalcin, thereby enhancing bone mineralization.[32] It may also inhibit osteoclastogenesis by increasing osteoprotegerin (OPG) expression and suppressing receptor activators of nuclear factor-κB ligand (RANKL), thus maintaining bone homeostasis.[33] However, we found that MK-4 could protect against bone loss by alleviating the impairment of type H vessels. Many studies have identified that angiogenesis and osteogenesis are closely coupled throughout bone development and remodeling.[15] Type H vessels play an active role in bone formation by secreting factors that promote proliferation and differentiation of bone progenitor cells within bone marrow.[15] Therefore, our result provided a new insight for understanding the mechanism of MK-4.

Previous studies have demonstrated that DM is marked by persistent elevated blood glucose, which can result in both macroangiopathy and microangiopathy.[34] Autophagy, a process by which cells utilize lysosomes to degrade damaged proteins and organelles, regulates metabolic energy balance and is crucial for bone regeneration.[35] It has been shown that MK-4 can induce osteoblast differentiation by promoting autophagy in MC3T3-E1 cells.[36] At the same time, MK-4 can upregulate osteoblasts' mitophagy inhibited by glucocorticoids, restoring osteoblast differentiation and mineralization. Our study found that MK-4 alleviates the impairment of type H vessels by promoting mitophagy. Our result align with a previous study, which found that MK-4 promotes osteogenic differentiation and mineralization of osteoblasts via upregulating mitophagy.[28] Given the critical role of mitophagy in the effect of MK-4, developing a hybrid drug containing mitochondrial targeting drugs and MK-4 will be more helpful for treating DOP.

Based on the above studies, we also look forward to exploring the specific mechanisms by which MK-4 regulates mitophagy in ECs. ERK is an activation signal derived from extracellular cues, and not only has extensive research highlighted the crucial role of ERK signaling in driving osteogenic differentiation as well as mineralization across the osteoblast spectrum,[37] but also that the regulation of osteoblast regeneration through a series of ERK activity waves.[38] Whereas there are minimal studies on whether MK-4 can affect the ERK pathway, VK_2 triggers cancer cell apoptosis in hepatocellular carcinoma and activates the MEK/ERK1/2 signaling pathway in a cell type-specific manner.[39] ERK 1/2 is also involved in regulating cellular autophagy. For example, DHA helps alleviate oxidative damage in the liver through the activation of mitophagy, which is mediated by the GPR120/ERK cascade signaling pathway. Furthermore, the well-studied PINK1/Parkin pathway is crucial in the regulation of mitophagy.[31] The above theories provide the possibility that MK-4 regulates EC autophagy through ERK signaling and no reports have yet

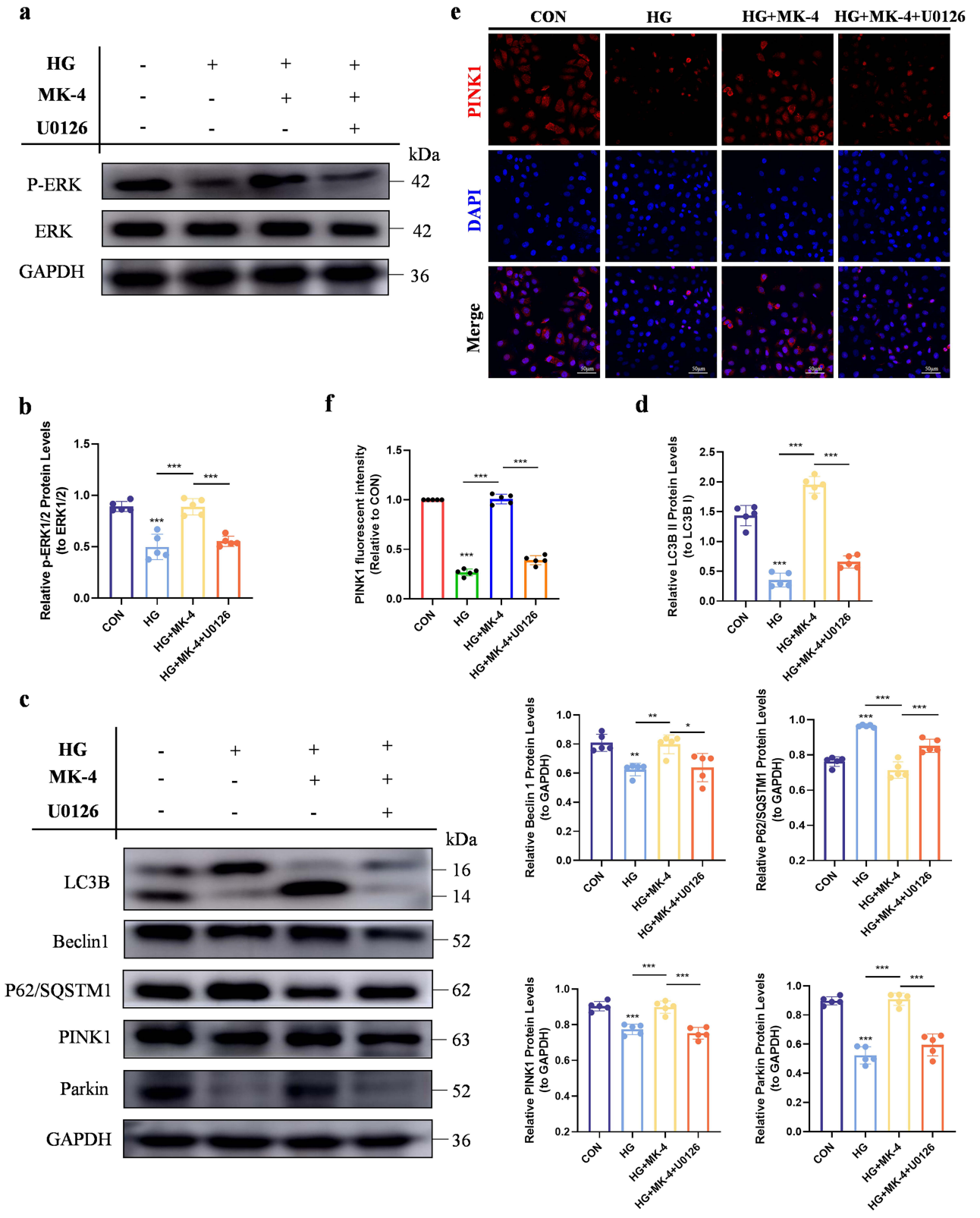

Figure 6 MK-4 promotes PINK1/Parkin-mediated mitophagy to alleviate ECs dysfunction via the ERK signaling pathway. (**a** and **b**) Western blotting assessment of p-ERK, ERK. (**c** and **d**) Western blotting assessment and statistic analysis of LC3B, Beclin 1, P62/SQSTM1, PINK1, and Parkin. (**e** and **f**) IF staining and statistic analysis of PINK1. Scale bar: 50μm. Data given as the mean±SD were representative of five independent experiments with similar results. *$P < 0.05$. **$P < 0.01$. ***$P < 0.001$.

https://doi.org/10.2147/DDDT.S503930

confirmed this. Therefore, current investigation innovatively revealed that inhibition of ERK 1/2 phosphorylation reduced MK-4-induced autophagosome formation or degradation, while eliminating MK-4-induced enhancement of PINK1 or Parkin expression, suggesting that ERK 1/2 is required for this process to function. It is recommended that MK-4 attenuates ECs dysfunction by promoting PINK1/Parkin-dependent mitophagy, potentially via ERK signaling pathway.

However, in this study, our research was limited to the promotion of angiogenesis by MK-4, which accelerated the bone formation rate. In the context of osteogenesis, the promotion of angiogenesis may only play a partial role, and the actual contribution of angiogenesis to bone formation remains to be further investigated. On the other hand, in this experiment, MK-4 was administered orally, and its mechanism of action involved absorption through the intestines and systemic circulation, exerting a whole-body effect. This experimental method lacks specificity, and aside from promoting local angiogenesis, MK-4 could potentially display anti-inflammatory properties by suppressing inflammatory pathways, including the nuclear factor κB (NF-κB) pathway, and reducing generation of other pro-inflammatory cytokines.[40] Additionally, MK-4 may promote osteogenesis by improving glucose metabolism, regulating insulin sensitivity and reducing the risk of type 2 diabetes, thus promoting metabolic health.[41] In future experiments, it is necessary to validate these effects by improving the method of drug administration.

In summary, DOP, as a chronic complication of diabetes in the skeletal system, seriously jeopardizes human bone health as well as increases the risk of fracture, therefore, prevention and treatment of DOP should draw public attention; however, its pathogenesis is complex and the current therapeutic options are limited. Our study focuses on the angiogenic disorders in the pathogenesis of DOP and investigates that MK-4 attenuates HG-induced ECs dysfunction, which in turn promotes angiogenesis-dependent bone formation in DOP mice, and reveals a novel mechanism by which MK-4 promotes PINK1/Parkin-dependent mitophagy via ERK signaling pathway (Figure 7). It will provide a novel insight into preventing DOP.

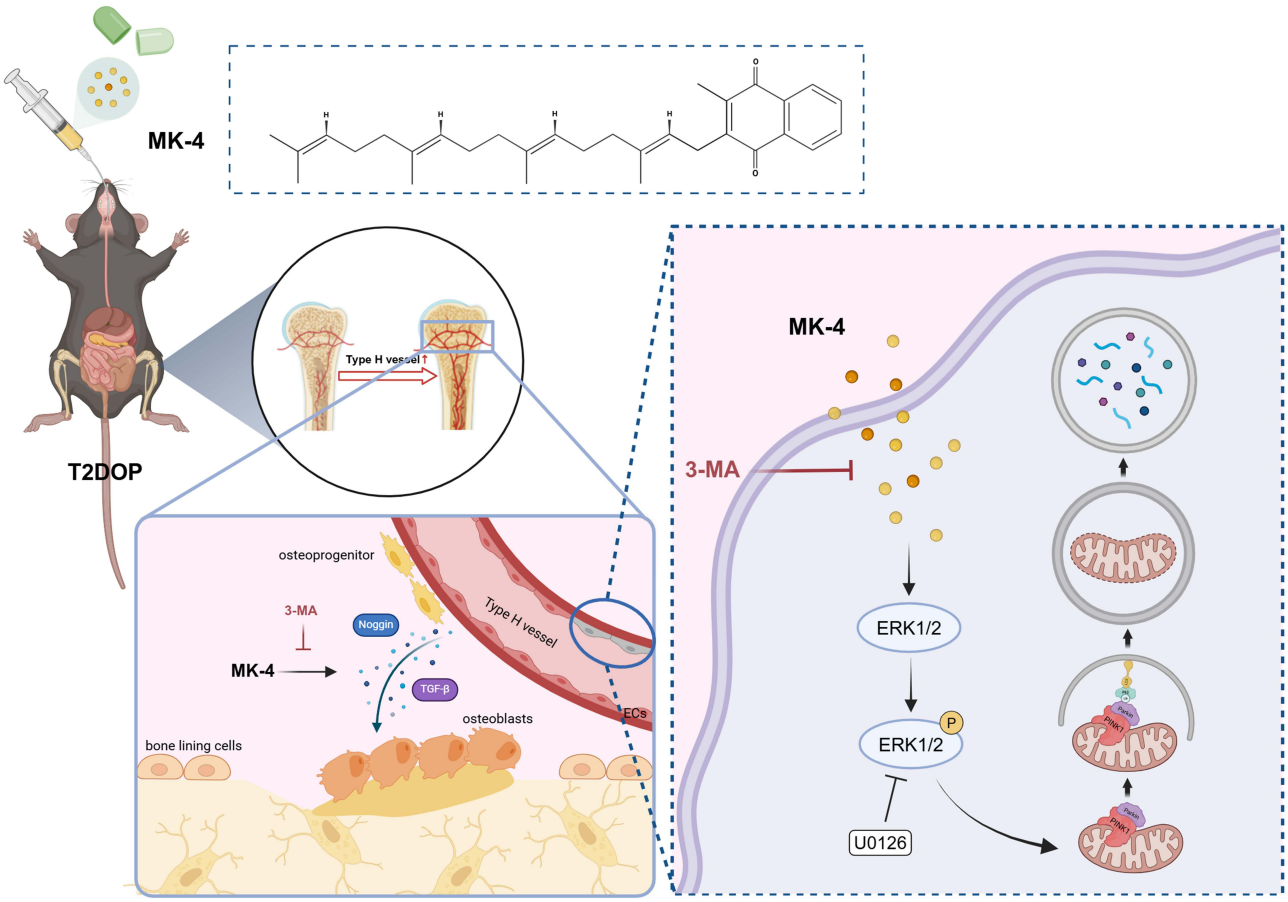

Figure 7 MK-4 ameliorates diabetic osteoporosis in angiogenesis-dependent bone formation by promoting mitophagy in endothelial cells.

Ethical Approval

All the animal procedures in this study were performed in accordance with the Guidelines for Care and Use of Laboratory Animals of the National Institutes of Health. Approval for all animal experiments was obtained from the Institutional Animal Care and Use Committee (IACUC) at the School and Hospital of Stomatology, Shandong University (No. 20230608).

Author Contributions

All authors made a significant contribution to the work reported, whether that is in the conception, study design, execution, acquisition of data, analysis and interpretation, or in all these areas; took part in drafting, revising or critically reviewing the article; gave final approval of the version to be published; have agreed on the journal to which the article has been submitted; and agree to be accountable for all aspects of the work.

Funding

This study was funded by the TaiShan Scholars of Shandong Province (No.tstp20221160) to Li M.

Disclosure

The authors declare that they have no conflicts of interest with the contents of this article.

References

1. Cole JB, Florez JC. Genetics of diabetes mellitus and diabetes complications. *Nat Rev Nephrol*. 2020;16(7):377–390. doi:10.1038/s41581-020-0278-5
2. Chen B, He Q, Yang J, et al. Metformin suppresses oxidative stress induced by high glucose via activation of the Nrf2/HO-1 signaling pathway in type 2 diabetic osteoporosis. *Life Sci*. 2023;312:121092. doi:10.1016/j.lfs.2022.121092
3. Seifu Y, Tsegaw D, Haji Y, Ejeso A. Prevalence and associated factors of diabetes mellitus among adult population in Hawassa Zuria Woreda, Sidama Region, Ethiopia. *Diabetes Metab Syndr Obes*. 2020;13:4571–4579. doi:10.2147/dmso.S275230
4. Hofbauer LC, Busse B, Eastell R, et al. Bone fragility in diabetes: novel concepts and clinical implications. *Lancet Diabetes Endocrinol*. 2022;10(3):207–220. doi:10.1016/s2213-8587(21)00347-8
5. Schousboe JT, Morin SN, Kline GA, Lix LM, Leslie WD. Differential risk of fracture attributable to type 2 diabetes mellitus according to skeletal site. *Bone*. 2022;154:116220. doi:10.1016/j.bone.2021.116220
6. Chen Y, Zhao W, Hu A, et al. Type 2 diabetic mellitus related osteoporosis: focusing on ferroptosis. *J Transl Med*. 2024;22(1):409. doi:10.1186/s12967-024-05191-x
7. Wu K, Wang P, Deng L, et al. Analysis of bone metabolic alterations linked with osteoporosis progression in type 2 diabetic db/db mice. *Exp Gerontology*. 2024;185:112347. doi:10.1016/j.exger.2023.112347
8. Rao P, Lou F, Luo D, et al. Decreased autophagy impairs osteogenic differentiation of adipose-derived stem cells via Notch signaling in diabetic osteoporosis mice. *Cell Signalling*. 2021;87:110138. doi:10.1016/j.cellsig.2021.110138
9. Hamann C, Kirschner S, Günther KP, Hofbauer LC. Bone, sweet bone--osteoporotic fractures in diabetes mellitus. *Nat Rev Endocrinol*. 2012;8(5):297–305. doi:10.1038/nrendo.2011.233
10. Cortet B, Lucas S, Legroux-Gerot I, Penel G, Chauveau C, Paccou J. Bone disorders associated with diabetes mellitus and its treatments. *Joint Bone Spine*. 2019;86(3):315–320. doi:10.1016/j.jbspin.2018.08.002
11. Feng W, Liu S, Zhang C, Xia Q, Yu T, Zhu D. Comparison of cerebral and cutaneous microvascular dysfunction with the development of type 1 diabetes. *Theranostics*. 2019;9(20):5854–5868. doi:10.7150/thno.33738
12. Xu Y, Peng Y, Wu X, et al. VEGF-B prevents chronic hyperglycemia-induced retinal vascular leakage by regulating the CDC42-ZO1/VE-cadherin pathway. *FASEB J*. 2024;38(17):e70019. doi:10.1096/fj.202300987RR
13. Pepe M, Addabbo F, Cecere A, et al. Acute hyperglycemia-induced injury in myocardial infarction. *Int J mol Sci*. 2024;25(15):8504. doi:10.3390/ijms25158504
14. Qin Q, Lee S, Patel N, et al. Neurovascular coupling in bone regeneration. *Exp Mol Med*. 2022;54(11):1844–1849. doi:10.1038/s12276-022-00899-6
15. Peng Y, Wu S, Li Y, Crane JL. Type H blood vessels in bone modeling and remodeling. *Theranostics*. 2020;10(1):426–436. doi:10.7150/thno.34126
16. Zhang J, Pan J, Jing W. Motivating role of type H vessels in bone regeneration. *Cell Proliferation*. 2020;53(9):e12874. doi:10.1111/cpr.12874
17. Hu XF, Xiang G, Wang TJ, et al. Impairment of type H vessels by NOX2-mediated endothelial oxidative stress: critical mechanisms and therapeutic targets for bone fragility in streptozotocin-induced type 1 diabetic mice. *Theranostics*. 2021;11(8):3796–3812. doi:10.7150/thno.50907
18. Zhang T, O'Connor C, Sheridan H, Barlow JW. Vitamin K2 in health and disease: a clinical perspective. *Foods*. 2024;13(11). doi:10.3390/foods13111646
19. Shearer MJ, Okano T. Key pathways and regulators of vitamin K function and intermediary metabolism. *Annu Rev Nutr*. 2018;38:127–151. doi:10.1146/annurev-nutr-082117-051741
20. Wang H, Zhang N, Li L, Yang P, Ma Y. Menaquinone 4 reduces bone loss in ovariectomized mice through dual regulation of bone remodeling. *Nutrients*. 2021;13(8):2570. doi:10.3390/nu13082570
21. Guralp O, Erel CT. Effects of vitamin K in postmenopausal women: mini review. *Maturitas*. 2014;77(3):294–299. doi:10.1016/j.maturitas.2013.11.002

22. Iwasaki-Ishizuka Y, Yamato H, Murayama H, Ezawa I, Kurokawa K, Fukagawa M. Menatetrenone rescues bone loss by improving osteoblast dysfunction in rats immobilized by sciatic neurectomy. *Life Sci*. 2005;76(15):1721–1734. doi:10.1016/j.lfs.2004.12.001
23. Cui Y, Zhang W, Yang P, Zhu S, Luo S, Li M. Menaquinone-4 prevents medication-related osteonecrosis of the jaw through the SIRT1 signaling-mediated inhibition of cellular metabolic stresses-induced osteoblast apoptosis. *Free Radic Biol Med*. 2023;206:33–49. doi:10.1016/j.freeradbiomed.2023.06.022
24. Kieronska-Rudek A, Kij A, Bar A, et al. Phylloquinone improves endothelial function, inhibits cellular senescence, and vascular inflammation. *GeroScience*. 2024;46(5):4909–4935. doi:10.1007/s11357-024-01225-w
25. Bar A, Kus K, Manterys A, et al. Vitamin K(2)-MK-7 improves nitric oxide-dependent endothelial function in ApoE/LDLR(-/-) mice. *Vascu Pharmacol*. 2019;122-123:106581. doi:10.1016/j.vph.2019.106581
26. Zhang Y, Yin J, Ding H, Zhang C, Gao YS. Vitamin K2 ameliorates damage of blood vessels by glucocorticoid: a potential mechanism for its protective effects in glucocorticoid-induced osteonecrosis of the femoral head in a rat model. *Int J Biol Sci*. 2016;12(7):776–785. doi:10.7150/ijbs.15248
27. Chen J, Meng X. Aronia melanocarpa anthocyanin extracts improve hepatic structure and function in high-fat diet-/streptozotocin-induced T2DM mice. *J Agric Food Chem*. 2022;70(37):11531–11543. doi:10.1021/acs.jafc.2c03286
28. Chen L, Shi X, Weng SJ, et al. Vitamin K2 can rescue the dexamethasone-induced downregulation of osteoblast autophagy and mitophagy thereby restoring osteoblast function in vitro and in vivo. *Front Pharmacol*. 2020;11:1209. doi:10.3389/fphar.2020.01209
29. Rong X, Kou Y, Zhang Y, et al. ED-71 prevents glucocorticoid-induced osteoporosis by regulating osteoblast differentiation via notch and wnt/β-catenin pathways. *Drug Des Devel Ther*. 2022;16:3929–3946. doi:10.2147/dddt.S377001
30. Xu T, Dong Q, Luo Y, et al. Porphyromonas gingivalis infection promotes mitochondrial dysfunction through Drp1-dependent mitochondrial fission in endothelial cells. *Int J Oral Sci*. 2021;13(1):28. doi:10.1038/s41368-021-00134-4
31. Chen J, Wang D, Zong Y, Yang X. DHA protects hepatocytes from oxidative injury through GPR120/ERK-mediated mitophagy. *Int J mol Sci*. 2021;22(11). doi:10.3390/ijms22115675
32. Iwamoto J. Vitamin K_2 therapy for postmenopausal osteoporosis. *Nutrients*. 2014;6(5):1971–1980. doi:10.3390/nu6051971
33. Wu WJ, Kim MS, Ahn BY. The inhibitory effect of vitamin K on RANKL-induced osteoclast differentiation and bone resorption. *Food Funct*. 2015;6(10):3351–3358. doi:10.1039/c5fo00544b
34. Le T, Salas Sanchez A, Nashawi D, Kulkarni S, Prisby RD. Diabetes and the microvasculature of the bone and marrow. *Curr Osteoporosis Rep*. 2024;22(1):11–27. doi:10.1007/s11914-023-00841-3
35. Wang J, Zhang Y, Cao J, et al. The role of autophagy in bone metabolism and clinical significance. *Autophagy*. 2023;19(9):2409–2427. doi:10.1080/15548627.2023.2186112
36. Li W, Zhang S, Liu J, Liu Y, Liang Q. Vitamin K2 stimulates Mc3T3-E1 osteoblast differentiation and mineralization through autophagy induction. *Mol Med Rep*. 2019. doi:10.3892/mmr.2019.10040
37. Kim JM, Yang YS, Hong J, Chaugule S, Chun H, van der Meulen MCH. Biphasic regulation of osteoblast development via the ERK MAPK-mTOR pathway. *eLife*. 2022;11. doi:10.7554/eLife.78069
38. De Simone A, Evanitsky MN. Control of osteoblast regeneration by a train of Erk activity waves. *Feb*. 2021;590(7844):129–133. doi:10.1038/s41586-020-03085-8
39. Matsumoto K, Okano J, Nagahara T, Murawaki Y. Apoptosis of liver cancer cells by vitamin K2 and enhancement by MEK inhibition. *Int j Oncol*. 2006;29(6):1501–1508.
40. Shea MK, Booth SL, Massaro JM, et al. Vitamin K and vitamin D status: associations with inflammatory markers in the Framingham offspring study. *Am j epidemiol*. 2008;167(3):313–320. doi:10.1093/aje/kwm306
41. Choi HJ, Yu J, Choi H, et al. Vitamin K2 supplementation improves insulin sensitivity via osteocalcin metabolism: a placebo-controlled trial. *Diabetes Care*. 2011;34(9):e147. doi:10.2337/dc11-0551